C-BAND LINAC OPTIMIZATION FOR A RACE-TRACK MICROTRON

Yu.A. Kubyshin, UPC, Barcelona, Spain
D. Carrillo, L. Garcia-Tabares, F. Toral, CIEMAT, Madrid, Spain
A.V. Poseryaev, V.I. Shvedunov, SINP MSU, Moscow, Russia

Abstract

Optimization results of a C-band standing wave biperiodic on-axis coupled linac for a miniature race-track microtron (RTM) are presented. The optimization procedure includes 2D cells geometry optimization to maximize the shunt impedance and minimize the surface field strength, choice of the linac cells number, length and field strength following requirements of the RTM beam dynamics and full scale 3D calculations.

INTRODUCTION

Miniature 12 MeV RTM for medical applications is under construction at UPC Barcelona in collaboration with several Spanish entities and SINP MSU (Russia) [1].

RTM dimensions are strongly dependent on its bending magnet field B_0, and because of $B_0 \sim 1/\lambda$ dependence, on the operating wavelength, λ. In previous optimization [1,2], wavelength λ=5.24 cm (frequency f = 5712 MHz) was chosen as optimal, providing minimal RTM dimensions at 12 MeV (maximum beam energy) and 2 MeV energy gain per turn.

Standing wave C-band linacs for industrial and medical applications were proposed in [3]. The first C-band linac in recirculating accelerator is successfully used at MAMI-C double sided microtron for acceleration of highly relativistic electron beams [4].

The peculiarity of RTM linac optimization is related to the necessity to provide a good capture efficiency for the non-relativistic electron beam at injection and efficient acceleration of relativistic beams at the subsequent orbits. The change of the wavelength from the S-band, at which all pulsed RTMs built till now are operating, to the C-band complicates the optimization procedure, this is due to the decrease of the energy gain per cell (cells are two times shorter) and so to increase of the phase slip effect.

2D LINAC OPTIMIZATION

2D RTM linac optimization was done without taking into account coupling slots and involves the following basic steps: (1) optimization of a β=1 cell geometry with SUPERFISH [5] and definition of the geometry of $\beta < 1$ cells with different lengths; (2) beam dynamics optimization of linac parameters with RTMTRACE [6] for a 25 keV injected beam and for a relativistic beam with different number of $\beta = 1$ cells and different lengths and field amplitudes of the first $\beta < 1$ cell; (3) first $\beta < 1$ cell geometry optimization.

Regular $\beta = 1$ Cell

Parameters describing the geometry of the accelerating structure are presented in Fig. 1. Three parameters strongly influencing on the cell effective shunt impedance – the beam hole radius, the length of coupling cell and the wall thickness – were fixed at R_b = 4 mm, L_c = 1.75 mm and t = 1.9 mm, respectively, by the condition to minimize beam losses in RTM, decrease sensitivity of the coupling cell frequency with respect to its length and get an adequate cooling [7]. The distance between noses was chosen as a compromise between the electric field strength at the surface and effective shunt impedance. For the geometry fixed in this way the surface peak-to-average on axis electric field ratio is 4, the quality factor 11700 and the effective shunt impedance 108 MOhm/m (without correction for coupling slots).

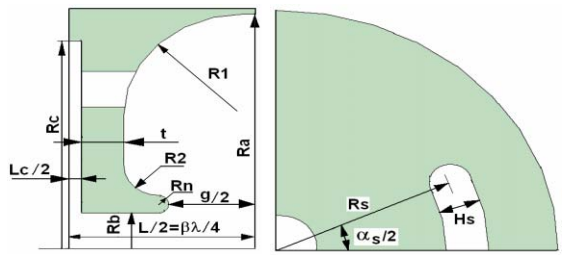

Figure 1: Geometry of the accelerating structure.

With the $\beta = 1$ cell geometry fixed and by adjusting relevant parameters a set of $0.4 < \beta < 0.8$ cell geometries were defined which were used in further beam dynamics simulations.

Beam Dynamics

To provide an efficient capture of a 25 keV beam from an electron gun and its acceleration to ~2 MeV the first linac cell must be made short enough and its field amplitude sufficiently high. The accelerated beam is reflected back by an RTM end magnet to the linac axis and must be accelerated then in the opposite direction to ~4 MeV [1]. The subsequent orbit beams with energy 4, 6, 8 and 10 MeV are accelerated in the same direction.

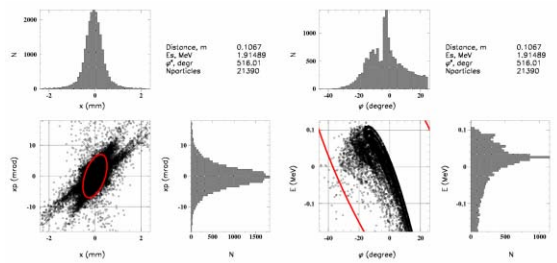

(a) (b)

Figure 2: Transverse (a) and longitudinal (b) phase space at linac exit.

* Work supported by the grants RDITSCON07-1-0015 of CIDEM (Catalonia, Spain) , 08-02-00273 of RFBR (Russia) and of CIEMAT.

Beam dynamics simulation was done for different number of β=1 cells, different lengths and field amplitudes of the $\beta < 1$ cell. For each variant the field amplitude was adjusted to provide the energy gain 2 MeV at the synchronous phase 16^0 for the relativistic beam. The following beam parameters were controlled at the linac exit for the 25 keV injected beam: energy, phase and energy spread, rms radius and divergence.

As a result of this study the following optimal structure of the linac was obtained: one $\beta = 0.5$ cell (first cell) followed by three $\beta = 1$ cells. The field amplitude in the first cell is 43 MV/m and the one in the $\beta = 1$ cells is 44.8 MV/m. In Fig. 2 the transverse and longitudinal phase space at linac exit is shown for the 25 keV injected beam.

First $\beta < 1$ Cell Geometry

The geometry of $\beta = 1$ cell scaled to $\beta = 0.5$ leaves no space for noses. The cell quality factor and effective shunt impedance turn out to be so low, that in order to produce the required field amplitude an essential part of RF power directed to the linac would be dissipated in the first cell. To increase the first cell quality factor its volume was enlarged by making it asymmetrical with respect to the central plane as it is shown in Fig. 3. The electric field peak-to-average ratio for this cell is 5.3 and quality factor is 8500.

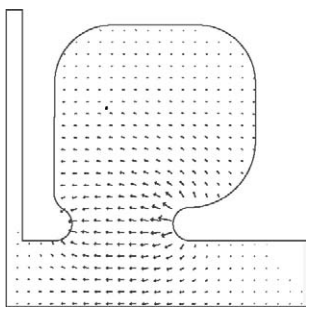

Figure 3: Electric field distribution within the volume of the first cell.

3D OPTIMIZATION

The goals of 3D simulation are: (1) coupling slot parameters R_s, H_s, α_s (Fig. 1) optimization for $\beta = 1$ cell to provide a high coupling factor with a reasonable drop in the effective shunt impedance by adjusting the first cell coupling slot angle α_s in order to reproduce the on-axis field distribution found in the beam dynamics simulation; (2) estimation of the RF power losses in each cell and total RF power required for design energy gain per turn; (3) calculation of linac - feeding waveguide coupling window parameters. The geometry of the assembled linac with a waveguide used in the calculations is shown in Fig. 4. 3D calculations were done independently by two groups using ANSYS [8] and HFSS [9] codes with a good agreement of the results.

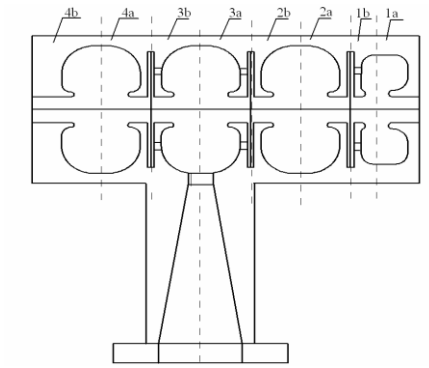

Figure 4: Axial section of the accelerating structure.

Coupling Slots Calculation

In Fig. 5 the assemblies used for $\beta = 1$ and first $\beta < 1$ cells calculations with coupling slots are shown. For several sets of coupling slot parameters the accelerating and coupling $\pi/2$ mode frequencies were tuned to 5712 MHz by changing the cell radii (R_a and R_c at Fig. 1) and the coupling factor was estimated. In this calculation the electric and magnetic wall boundary conditions at the axial boundary planes for the $\beta = 1$ cell were imposed. A similar procedure was carried out for the first $\beta < 1$ cell and the $\beta = 1$ end cell, in this case with a control of the on-axis field distribution. Coupling factor obtained for $\beta = 1$ cells is 10.6%.

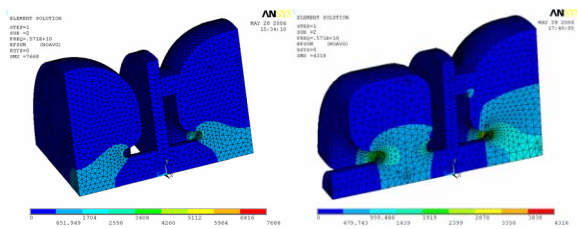

(a) (b)

Figure 5: Assemblies used for (a) $\beta = 1$ cell and (b) first $\beta < 1$ cell calculations with coupling slots (ANSYS).

At the next step the whole assembly without feeding waveguide was calculated, the obtained field distribution is shown in Figs. 6 and 7.

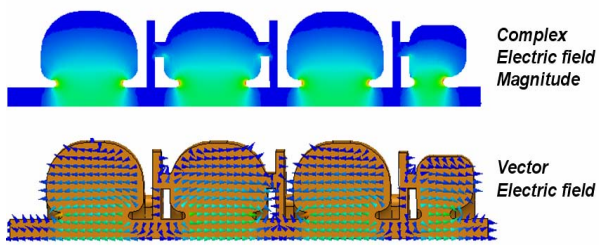

Figure 6: Electric field in the structure without feeding waveguide (HFSS).

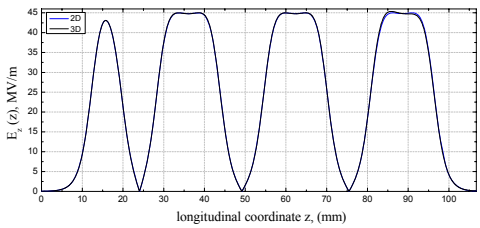

Figure 7: Comparison between 2D and 3D on-axis field distribution.

As it can be seen from Fig. 7 the on-axis field distribution obtained in the 3D calculations with the optimized coupling slots reproduces with a good accuracy the required field found in the beam dynamics simulation. The main characteristics of the accelerating structure are summarized in Table 1.

Table 1: Main characteristics of the accelerating structure.

Resonant frequency (π/2 - mode), f (MHz)	5712
Quality Factor, Q_0	9860
Total pulsed RF power dissipated in the structure walls, P_{RF} (kW)	600

Linac Coupling With Waveguide

The coupling factor of the feeding waveguide with linac for our scheme of the magnetron frequency synchronization is determined by the linac beam loading. For the design under consideration the pulsed current at 12 MeV is I_p=5 mA, maximum pulsed beam power is $P_b \approx 60$ kW, while the pulsed RF power dissipated in the structure walls is $P_w \approx 600$ kW. Therefore, in order to get zero reflected power at the steady state in resonance the coupling factor must be equal to $\beta_c \approx 1+P_b/P_w=1.1$. Taking into account the beam power losses and quality factor decrease due to surface imperfections for these simulations we chose the coupling factor $\beta_c \approx 1.2$ - 1.3. Fig. 8 shows the model used in the calculation of the coupling factor with HFSS code.

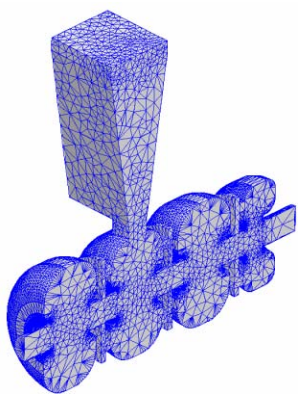

Figure 8: Half structure simulated with coupling window

During calculations S_{11} parameter,

$$S_{11} = 20\log\left|\frac{\beta_c - 1}{\beta_c + 1}\right|,$$

was optimized by adjusting the length of the coupling window with simultaneous adjustment of the coupler accelerating cell radius to compensate its resonance frequency shift. An example of the dependence of S_{11} on the resonance frequency is shown in Fig. 9. As the result of the calculations the coupling window length which provides $\beta_c \approx 1.2$ was found to be 13.2 mm.

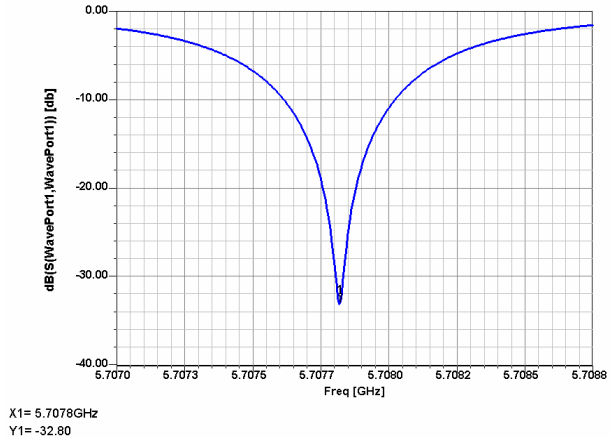

Figure 9: Example of S_{11} parameter dependence on resonance frequency in HFSS calculations.

CONCLUSIONS

A compact standing wave bi-periodic on-axis coupled accelerating structure for a RTM was optimized in the C-band. All parameters necessary for the linac engineering design were fixed. The linac is under construction now.

REFERENCES

[1] A.V. Poseryaev et al., In Proc. of EPAC 2006, p. 2340
[2] B.S. Ishkhanov et al., in Proc. RuPAC 2004, p. 474
[3] E. Tanabe et al., in Proc. Linac 98, p. 627, Ch. Tang et al., in Proc. LINAC 2006, p. 256, S. H. Kim et al., in Proc. APAC 2007, p. 442, in Proc. PAC 2007, p. 2823
[4] A. Jankowiak et al., in Proc. EPAC 2006, p. 834
[5] http://laacg1.lanl.gov/laacg/services/
[6] V.G. Gevorkyan et al., RTMTRACE, preprint VINITI 678-88 (1988)
[7] H. Euteneuer et al, in Proc. EPAC 2000, p. 1956
[8] http://www.ansys.com/
[9] http://www.ansoft.com/hfss/